Electronic Supplementary Material (ESI) for Journal of Materials Chemistry B.

Supporting Information

A Novel Peptide Targeting c-Met for Hepatocellular Carcinoma Diagnosis

Yongjia Tang[1#], Haoran Xu[1#],Yaxue Dai[1], Fang Wang[1], Wenjing Huang[1], Peifei Liu[1], Yueqing Gu[1*]

[1] State Key Laboratory of Natural Medicine, Department of Biomedical Engineering, School of Engineering, China Pharmaceutical University, No. 24 Tongjia Lane, Gulou District, Nanjing 211198, China

[#] First authors: These authors contributed equally to the work. Yongjia Tang and Haoran Xu, Email: wz712tyj@163.com (Y.T), xuhaoran123456@126.com (H.X).

[*] Corresponding author: Prof. Yueqing Gu, Ph.D. Email: guengineering@cpu.edu.cn.

Design and Screening of c-Met-Targeting Peptides

We aim to utilize structure-based virtual simulation strategy to obtain a targeting peptide for identifying c-Met. We have noticed that GE137 was folded into beta sheet by double disulfide bond, and the sequence between the Cys4 and Cys16 played a critical role in interacting with the Sema domain (PDB ID:1SHY) of c-Met (Fig S1). We designed a virtual peptide library based on the sequence between the double disulfide bond of GE137, and the Discovery studio 2016 softwre was used to analyze the interaction between peptides and Sema domain of c-Met (Table S1). The results showed that the highest affinity binding with c-Met were YQ-M3, YQ-M6 and YQ-M7, and the three peptides were selected for further study.

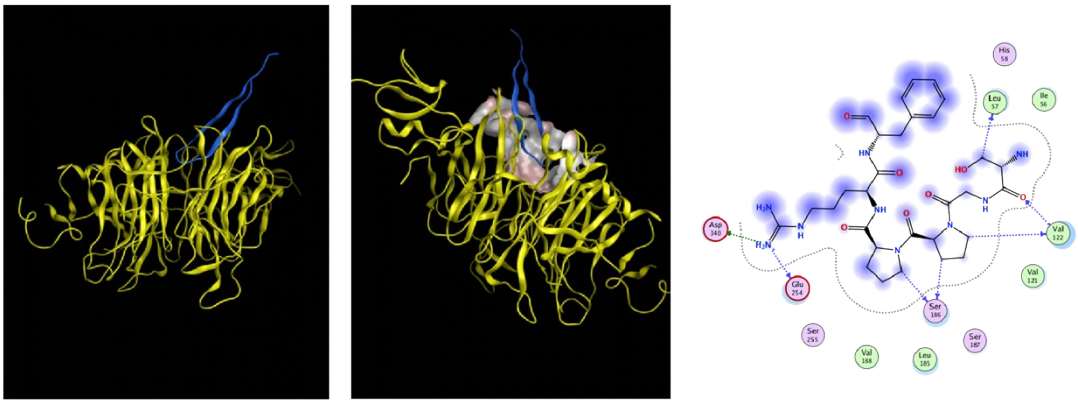

Fig S1. Molecular docking and interaction analysis of GE137 binding with Sema domain of c-Met.

Table S1. Virtual screening of designed peptides

name	Sequences	Score
YQ-M1	CYCSG	122.179
YQ-M2	YCSGP	144.199
YQ-M3	YGPPR	169.45
YQ-M4	CSGPP	152.876
YQ-M5	CGPPR	156.534
YQ-M6	SGPPR	161.31
YQ-M7	GPPRF	160.861
YQ-M8	PPRFE	153.227
YQ-M9	PRFEC	150.17
YQ-M10	RFECW	113.099
YQ-M11	FECWC	121.795

YQ-M3, YQ-M6 and YQ-M7 were labeled with near-infrared fluorescent dye MPA to build NIR probes, and flow cytometry was used to evaluate the binding ability between YQ-M3-MPA, YQ-M6-MPA, YQ-M7-MPA and c-Met positive HCC cell lines (HepG2) in a physiological environment (Fig. S2). The results showed that the affinity between YQ-M3-MPA and HepG2 cells was the highest. Therefore, YQ-M3

was chosen in our study for hepatocellular carcinoma diagnosis.

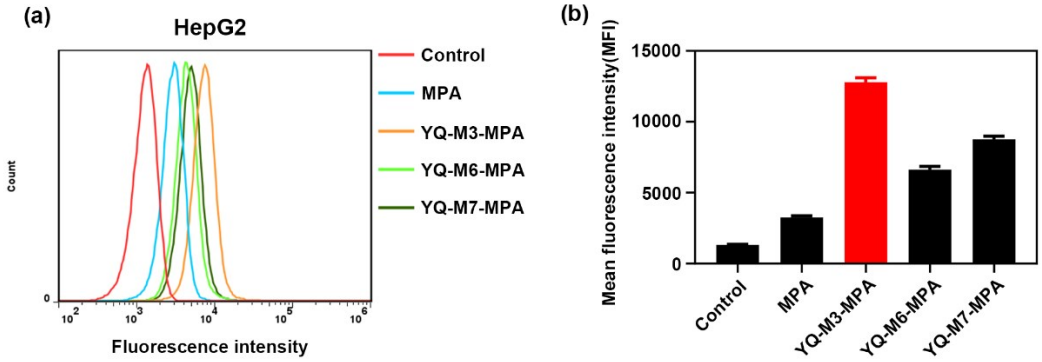

Fig S2. Binding affinity analysis of HepG2 cells incubated with YQ-M3-MPA, YQ-M6-MPA and YQ-M7-MPA, free MPA used as negative control.

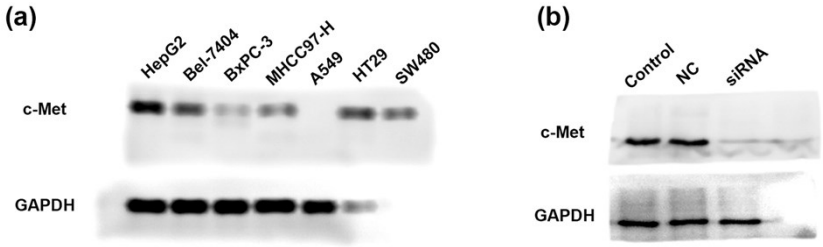

Fig.S3-1. (a) Western blot of the c-Met expression on different cells. (b) c-Met expression after transfection with c-Met siRNA or NC.

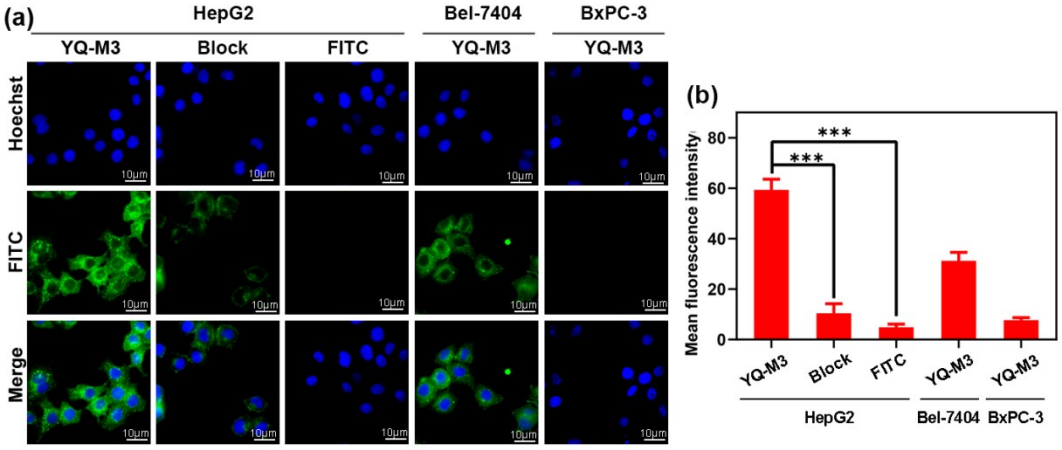

Fig.S3-2. (a) Cellular localization imaging analysis by inverted fluorescence microscopy images of HepG2, Bel-7404 and BxPC3 cells treated with YQ-M3-FITC, and FITC group and block group were added in HepG2 cells. (b) Semi-quantification mean fluorescence intensity of the corresponding fluorescence images(***$P < 0.01$).

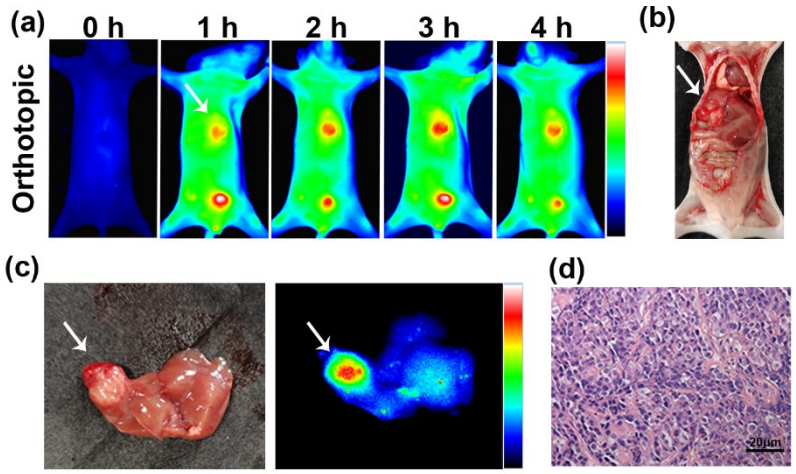

Figure S4. Near-infrared fluorescence imaging of orthotopic xenograft HepG2 tumor model. (a) In vivo imaging of YQ-M3-MPA in HepG2 orthotopic xenograft tumor mice. (b) Mice after NIR fluorescence imaging was sacrificed and dissected to confirm the presence of orthotopic liver tumors. The white arrow indicated the liver orthotopic xenograft tumor. (c) Ex vivo imaging of orthotopic liver tumors at the 4 h after injection. (d) H&E staining of the orthotopic liver tumor.

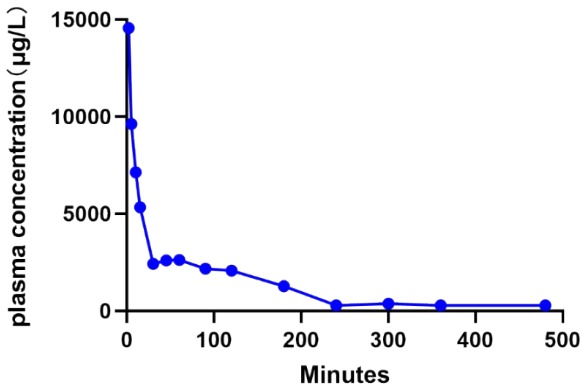

Figure S5. Plasma YQ-M3-MPA concentration−time profiles in rats following intravenous administration.

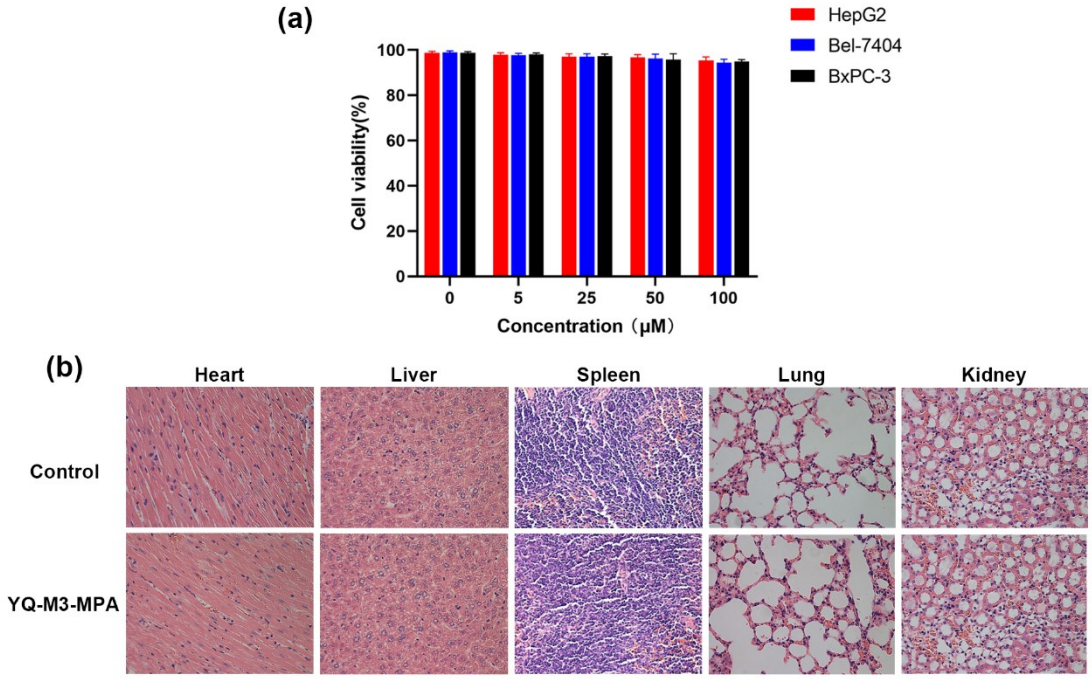

Figure S6. Cell viability assay in vitro and toxicity assay in vivo of YQ-M3-MPA. (a) The cell viability of YQ-M3-MPA in HepG2, Bel-7404 and BxPC-3 were examined by MTT assay. (b) Acute toxicity was tested in mice and H&E staining was used to stain the excised organs observed for H&E analysis.

MPA: 1H NMR (400 MHz, D2O) δ 8.76 (d, J = 13.7 Hz, 2H), 7.79 (s, 2H), 7.73 (d, J = 8.3 Hz, 2H), 7.27 (d, J = 8.4 Hz, 2H), 6.27 (d, J = 18.6 Hz, 2H), 4.20 (dd, J = 9.8, 4.8 Hz, 4H), 2.96 (t, J = 7.0 Hz, 5H), 2.82 (t, J = 7.1 Hz, 2H), 2.60-2.53 (m, H), 2.49 (t, J = 7.0 Hz, 2H), 2.36 (t, J = 7.0 Hz, 2H), 2.24-2.09 (m, 4H), 1.86-1.63 (m, 12H).

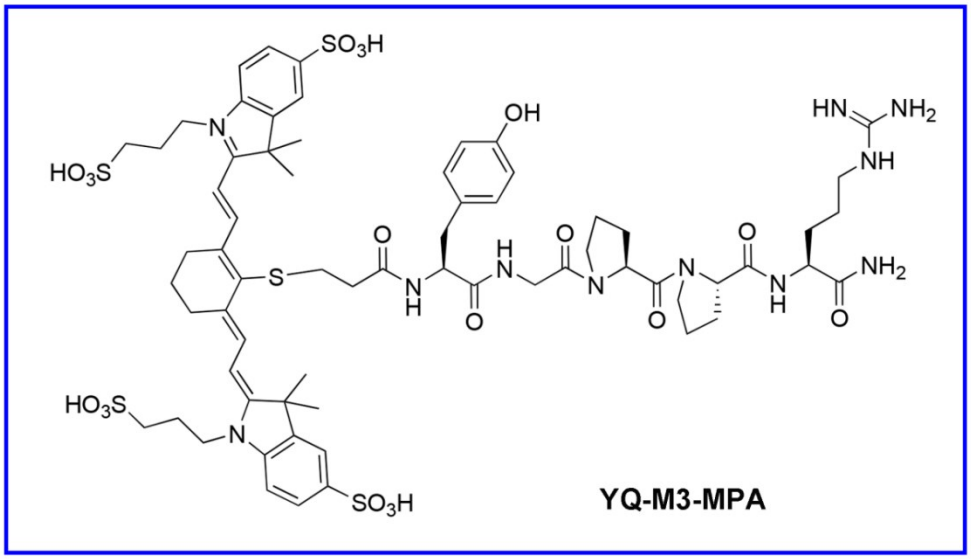

Figure S7-1. The chemical structures of YQ-M3-MPA

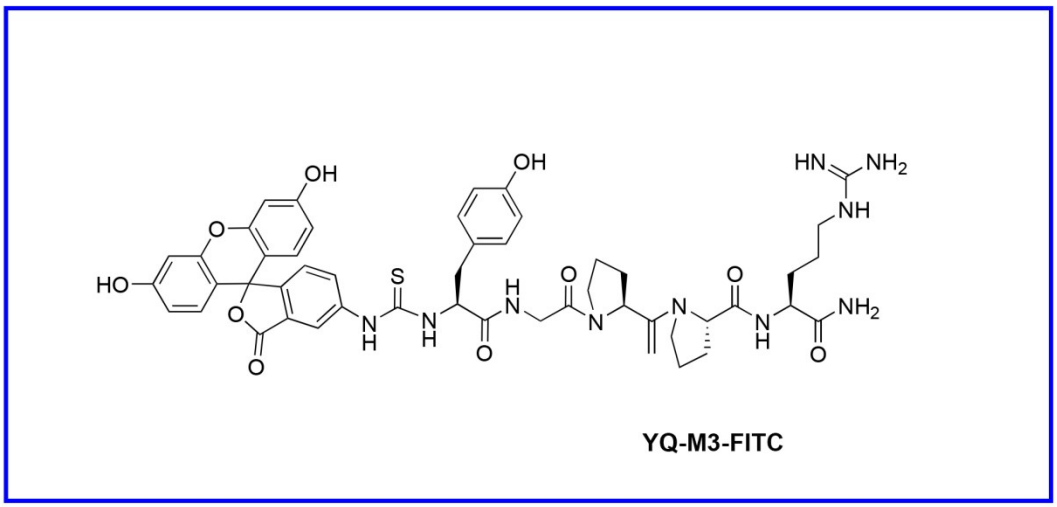

Figure S7-2. The chemical structures of YQ-M3-FITC

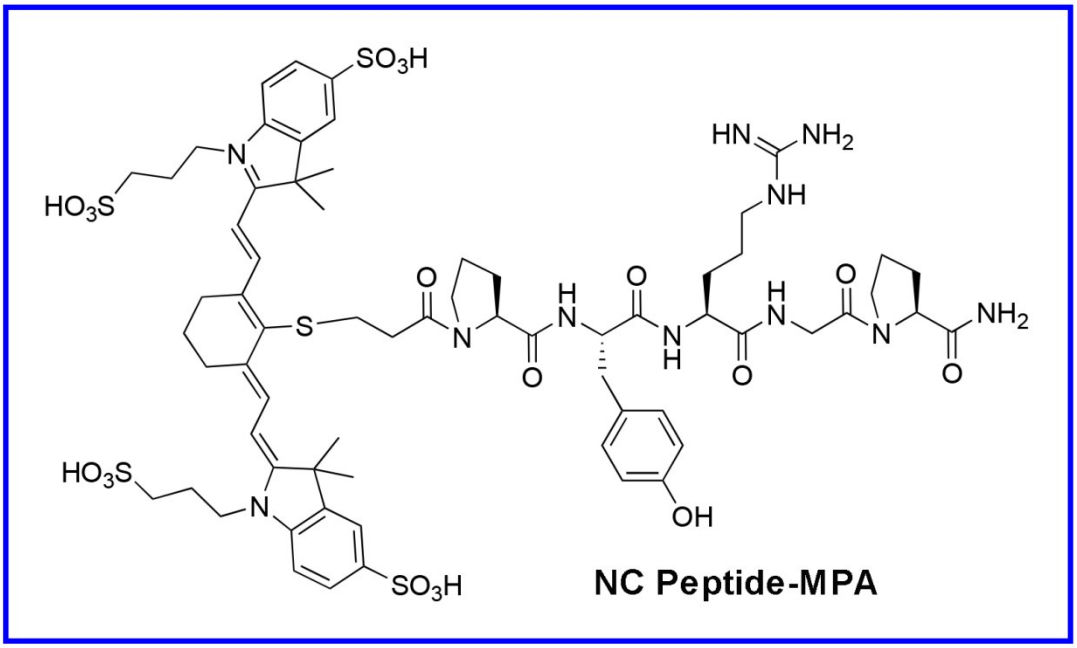

Figure S7-3. The chemical structures of nonsense control peptide-MPA

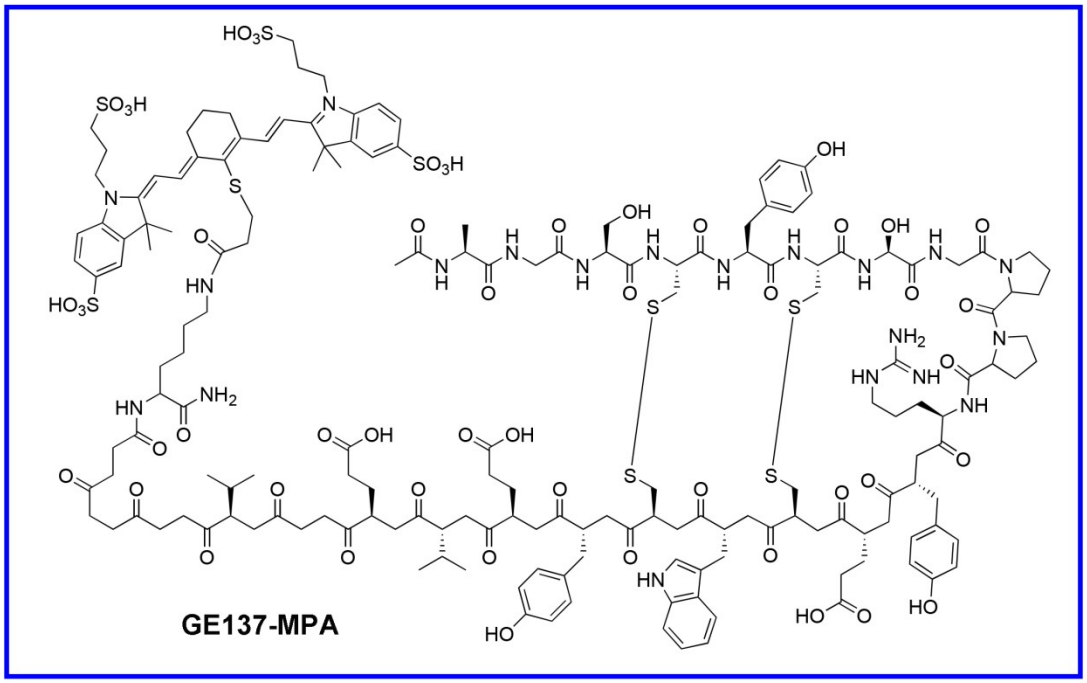

Figure S7-4. The chemical structures of GE137-MPA

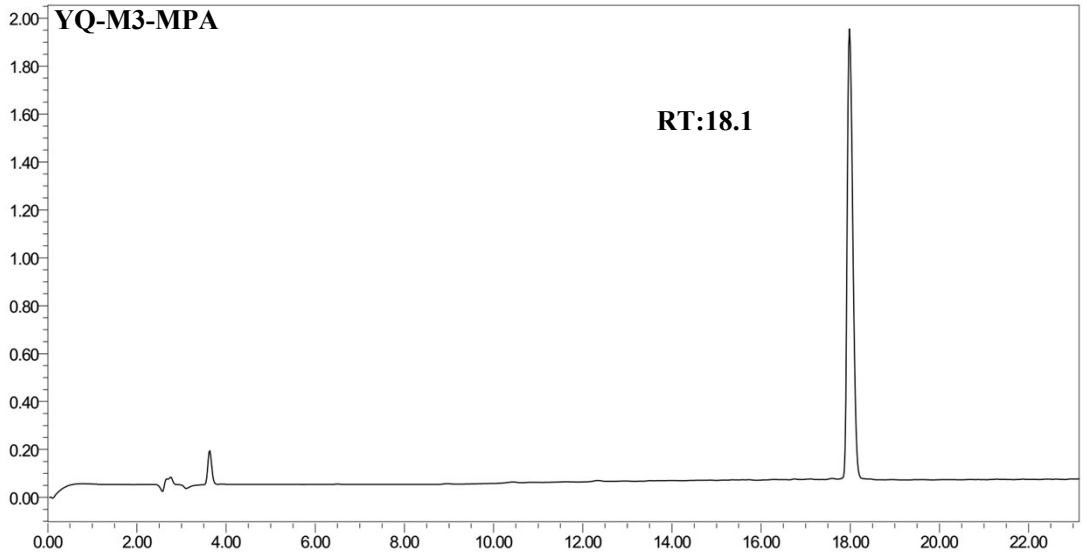

Figure S7-5. Typical HPLC chromate-gram of YQ-M3-MPA. (RT: retention time)

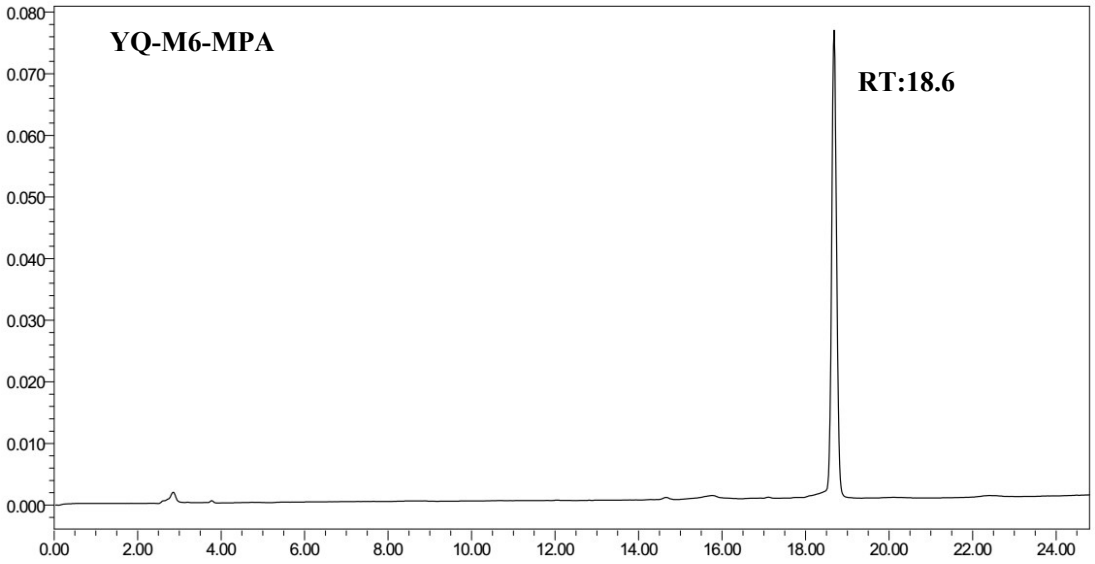

Figure S7-6. Typical HPLC chromate-gram of YQ-M6-MPA. (RT: retention time)

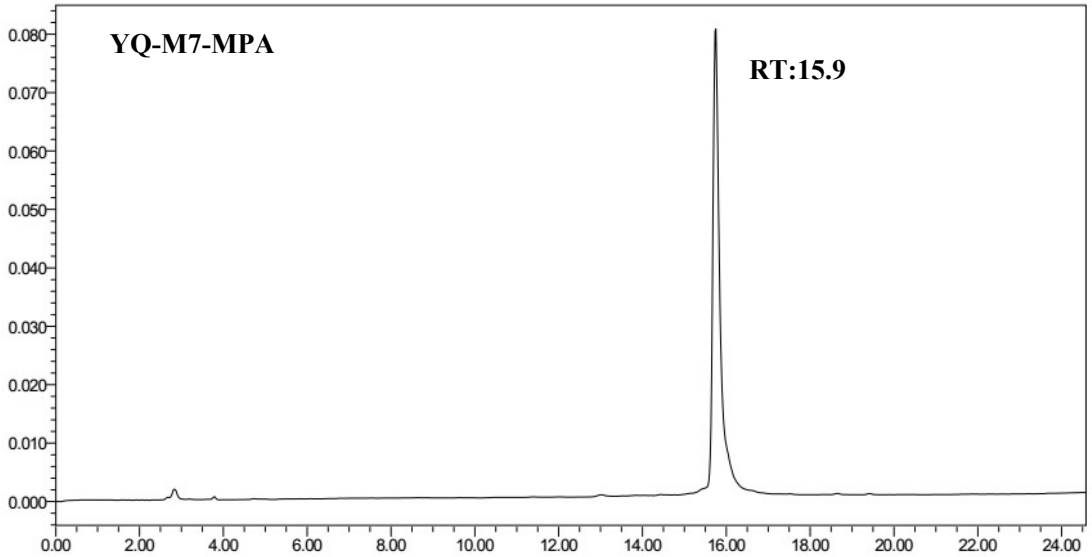

Figure S7-7. Typical HPLC chromate-gram of YQ-M7-MPA. (RT: retention time)

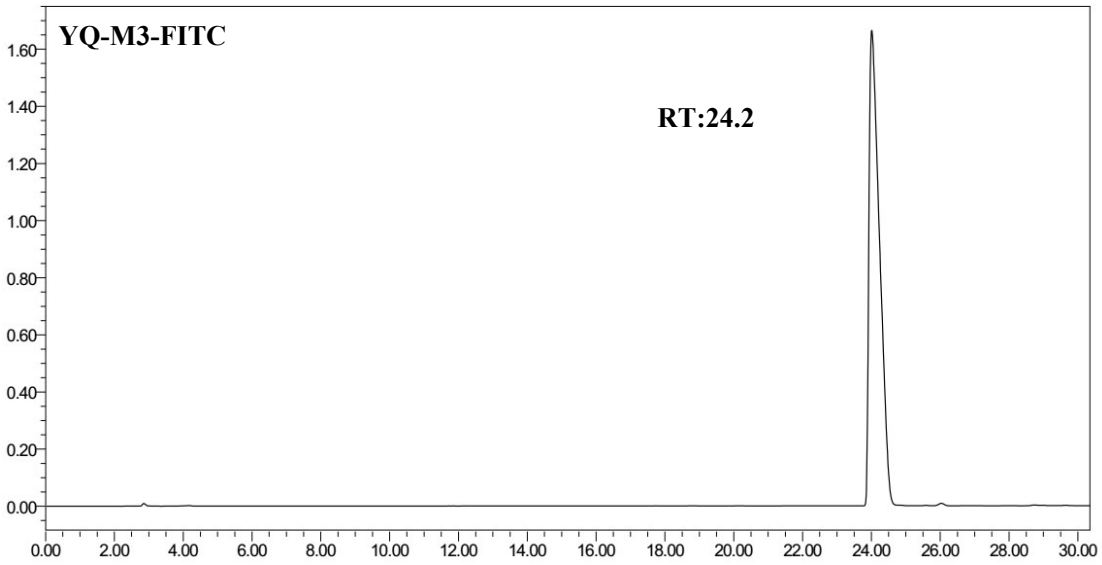

Figure S7-8. Typical HPLC chromate-gram of YQ-M3-FITC. (RT: retention time)

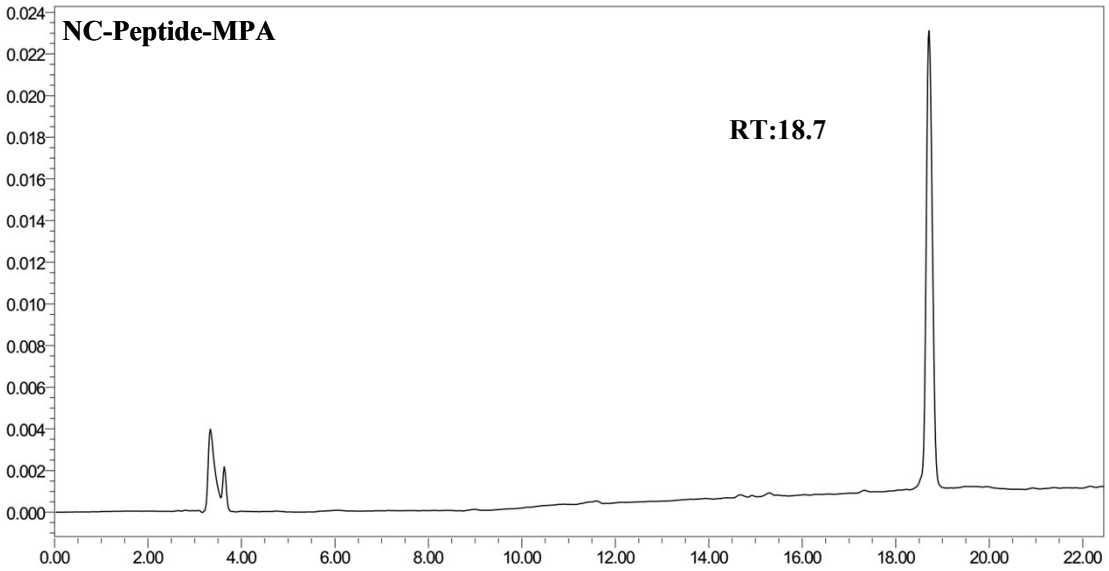

Figure S7-9. Typical HPLC chromate-gram of NC-Peptide-MPA. (RT: retention time)

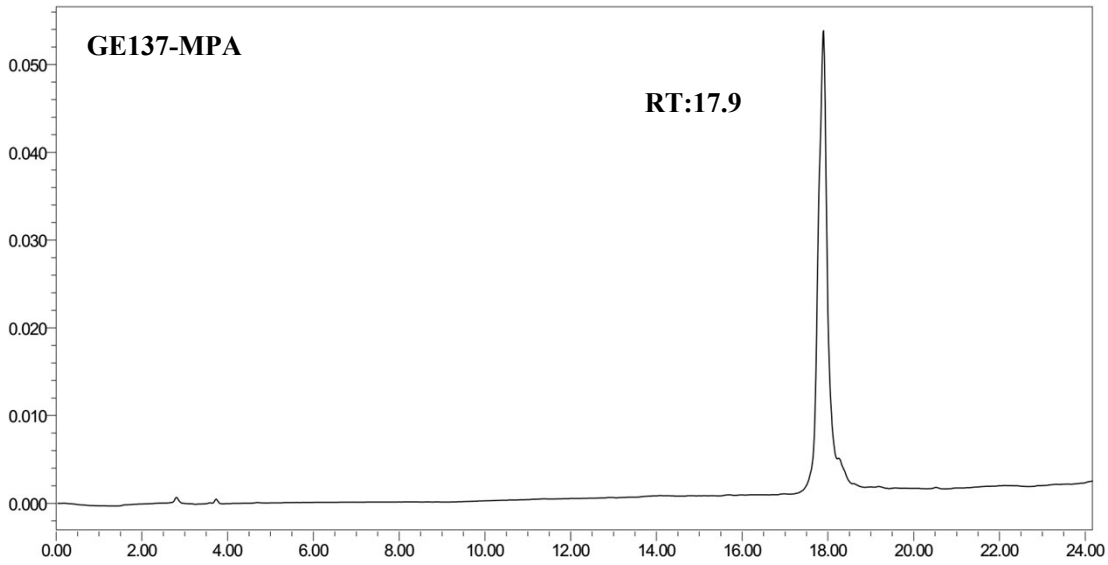

Figure S7-10. Typical HPLC chromate-gram of GE137-MPA. (RT: retention time)

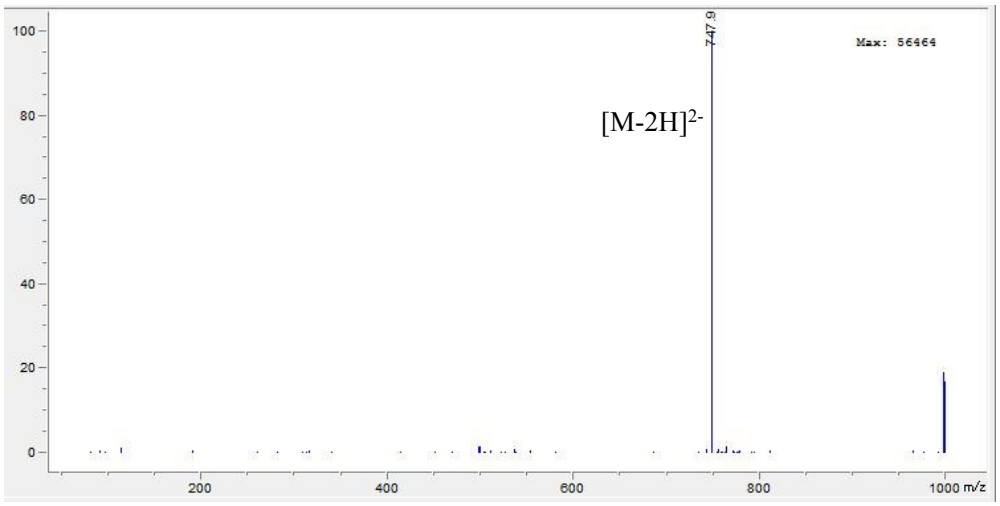

Figure S7-11. MS spectrum of YQ-M3-MPA.(MW:1498.2)

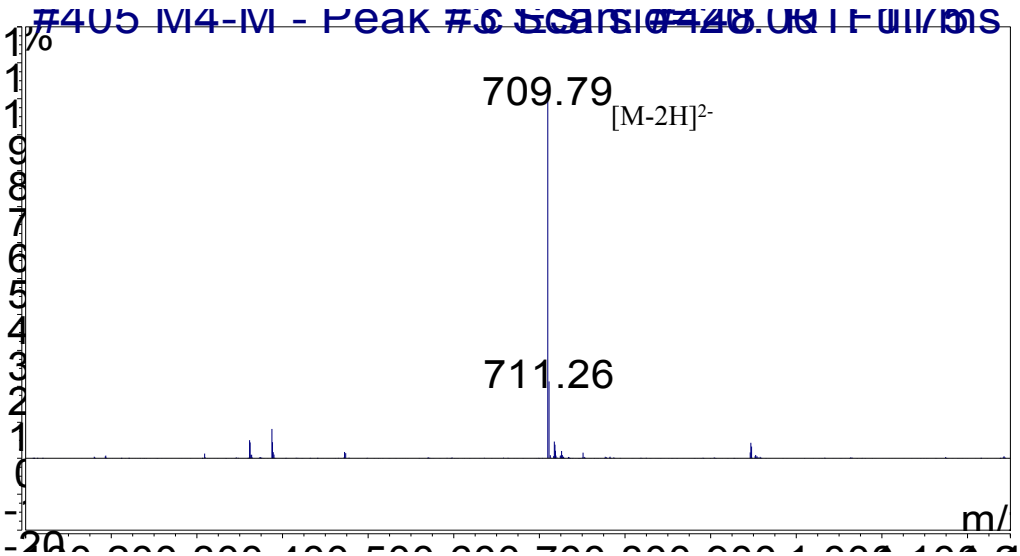

Figure S7-12. MS spectrum of YQ-M6-MPA.(MW:1422)

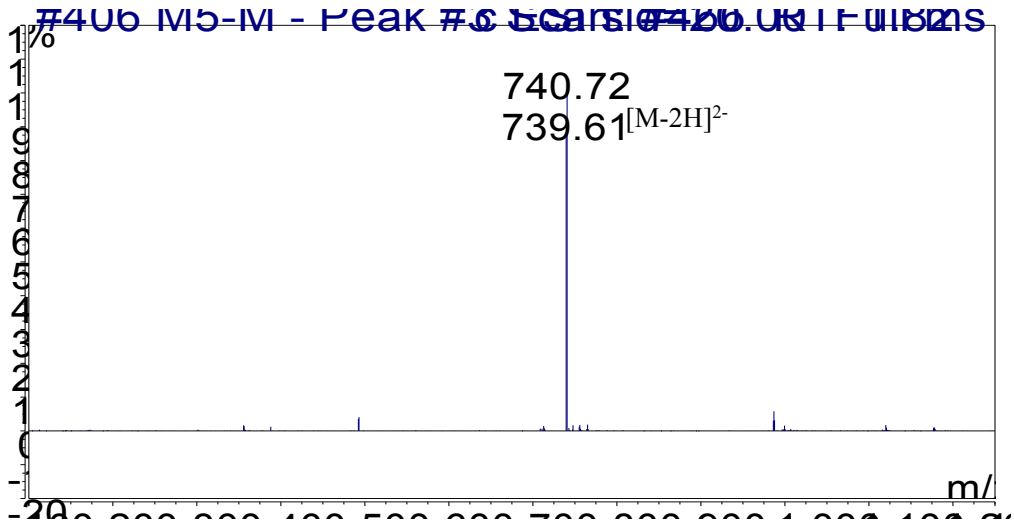

Figure S7-13. MS spectrum of YQ-M7-MPA.(MW:1482)

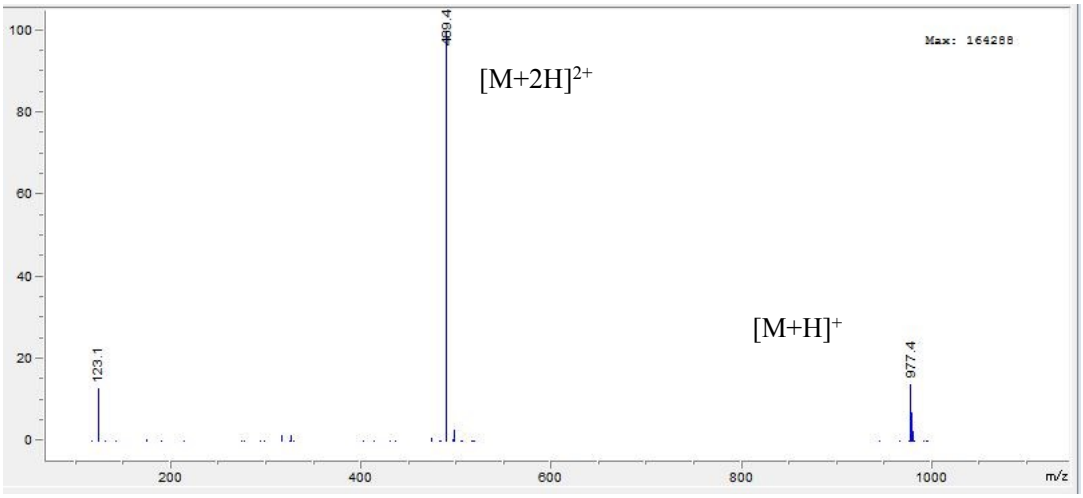

Fig S7-14. MS spectrum of YQ-M3-FITC.(MW:977.0)

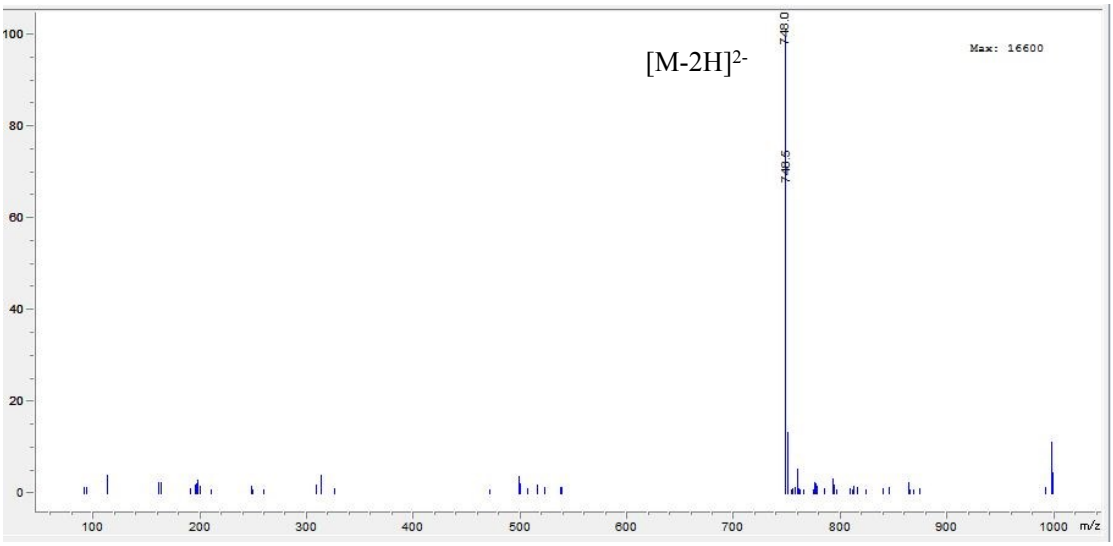

Fig S7-15. MS spectrum of NC-Peptide-MPA.(MW:1498.2)

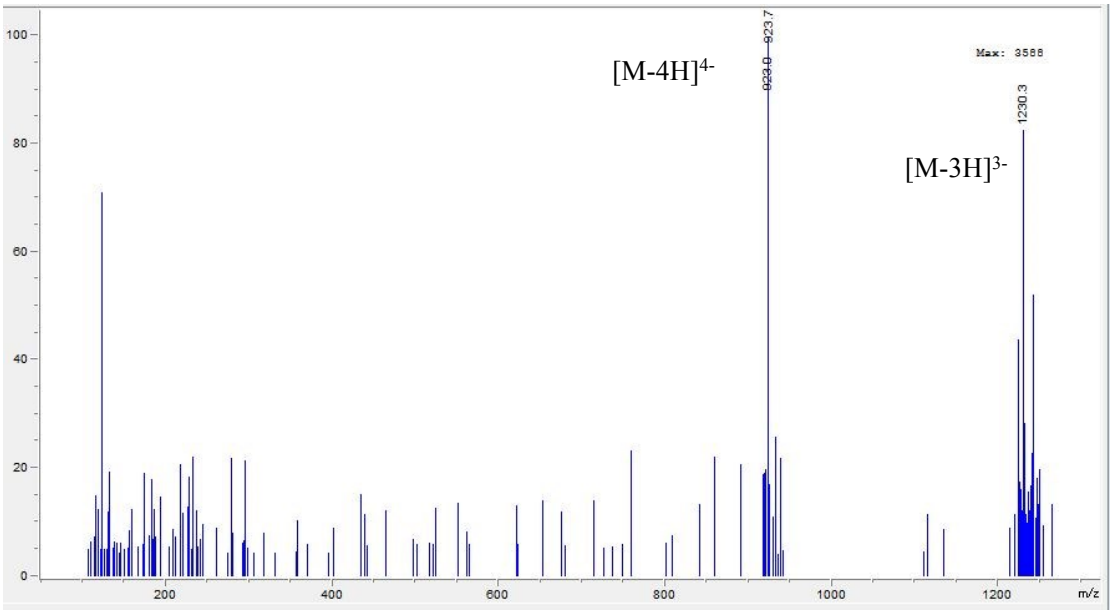

Fig S7-16. MS spectrum of GE137-MPA.(MW:3694.0)

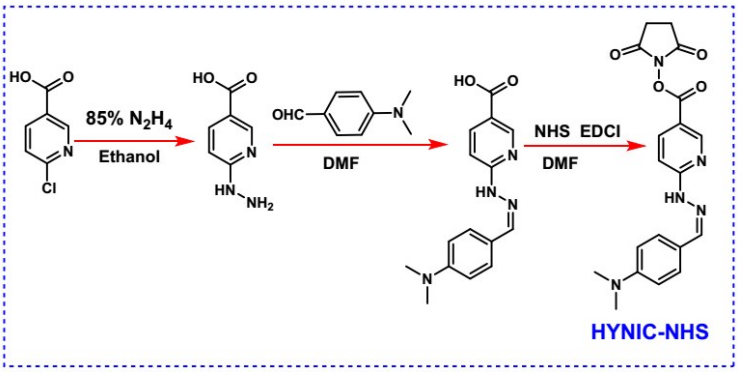

Fig S8-1. Structure and synthetic route of HYNIC-NHS

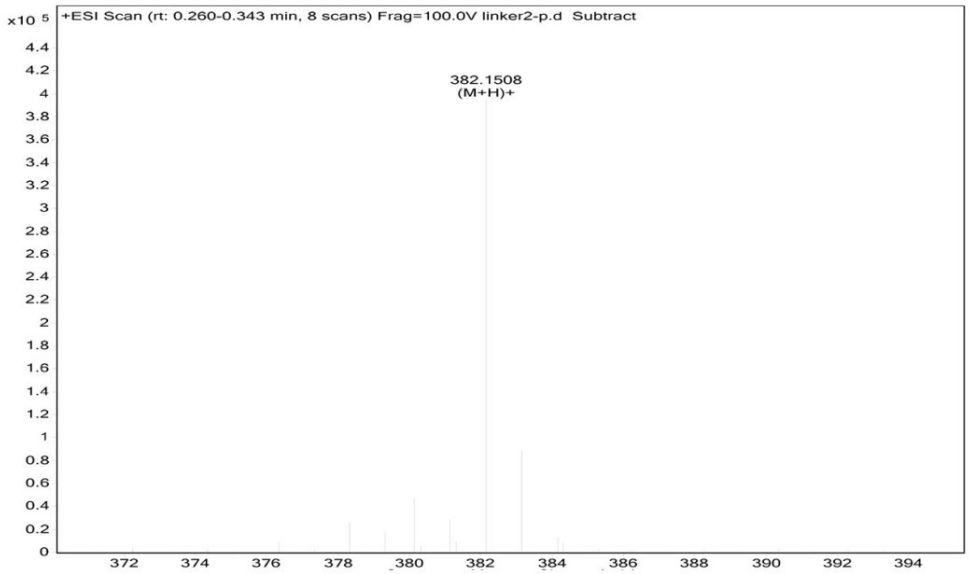

Fig S8-2. MS spectrum of HYNIC-NHS (MW:381.39)

HYNIC-NHS: 1H NMR (400 MHz, DMSO-d) δ 8.60 (s, 1H), 8.08 (d, J = 7.5 Hz, 1H), 7.99 (s, 1H), 7.51 (d, J = 7.3 Hz, 2H), 7.40 (d, J = 7.5 Hz, 1H), 6.71 (d, J = 7.6 Hz, 2H), 3.01 (s, 6H), 2.78 (s, 4H).

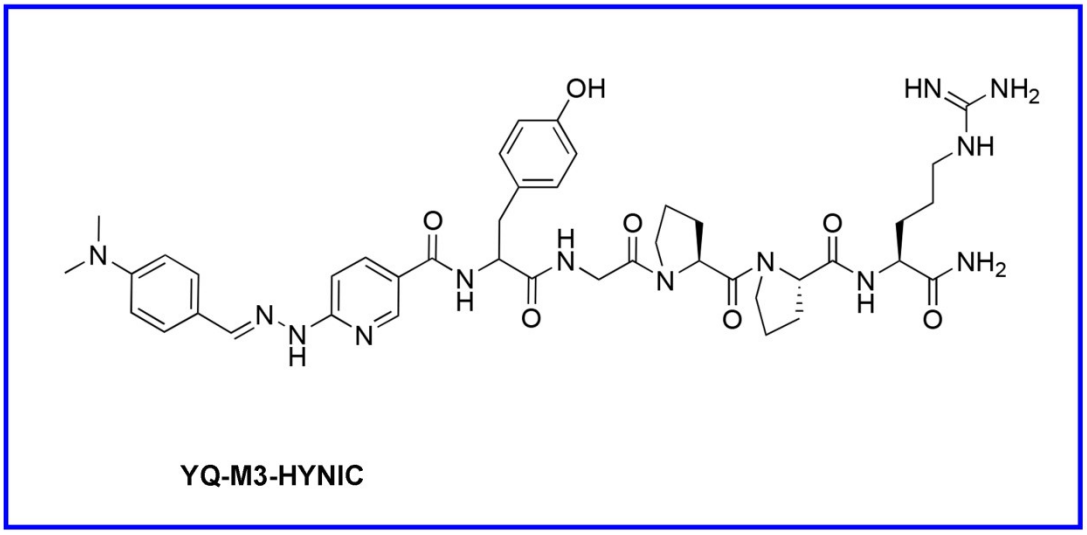

Fig S8-3. The chemical structures of YQ-M3-HYNIC

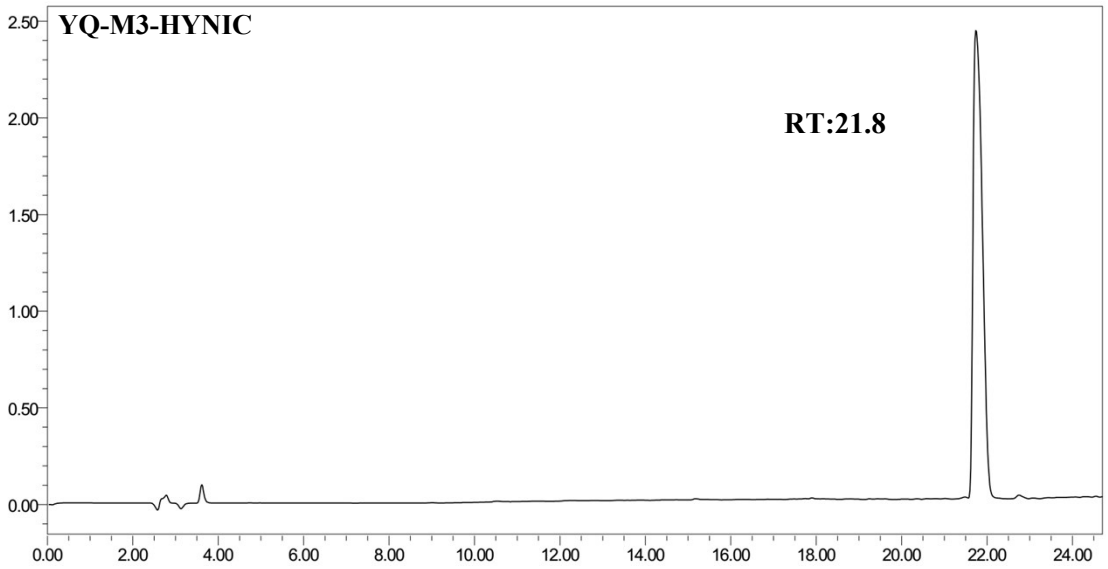

Fig S8-4. Typical HPLC chromate-gram of YQ-M3-HYNIC. (RT: retention time)

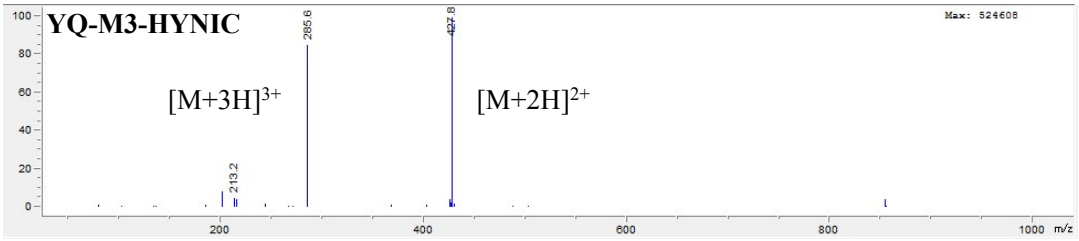

Fig S8-5. MS spectrum of YQ-M3-HYNIC (MW:853.6)

Radiochemistry

YQ-M3-HYNIC were prepared by direct conjugation of YQ-M3 with HYNIC-NHS (Figure S2-1). The products were confirmed by C18 analytical HPLC (purity>98%). The molecule weight of YQ-M3-HYNIC was corroborated by mass spectrometry ($[M+2H]^{2+}$=427.8 and ($[M+3H]^{3+}$=285.6) and matches with calculated value (853.6) (Figure S2-5). YQ-M3-HYNIC were radiolabeled with $Na^{99m}TcO_4$ through a reported method, using TPPTS and tricine as coligands to obtain highly stable complexes with a yield of >96% and specific activity of >25 GBq/μmol. Subsequent, the tracers were purified via a Sep-Pak C-18 column and improved the radiochemical purity of the tracers to >99%. The Radio-HPLC chromatography of the purified tracers are shown in Figure S2-7. The well-prepared probe was used for further experiments, without further purification.

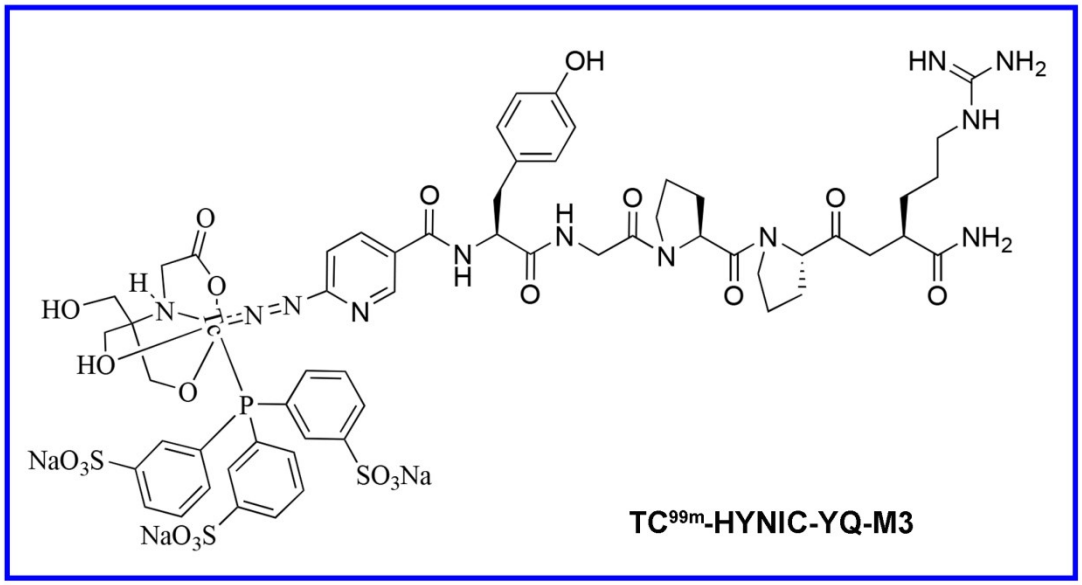

Figure S8-6. The chemical structures of YQ-M3-MPA

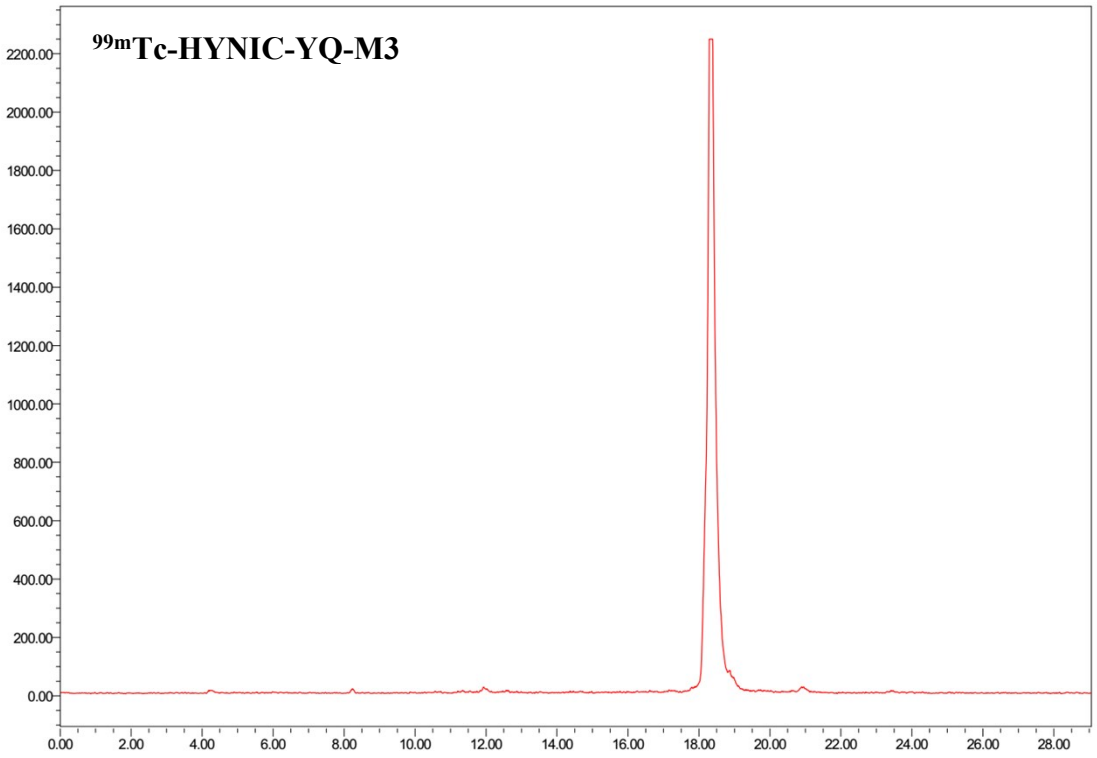

Figure S8-7. Typical radio-HPLC chromate-gram of ^{99m}Tc-HYNIC-YQ-M3

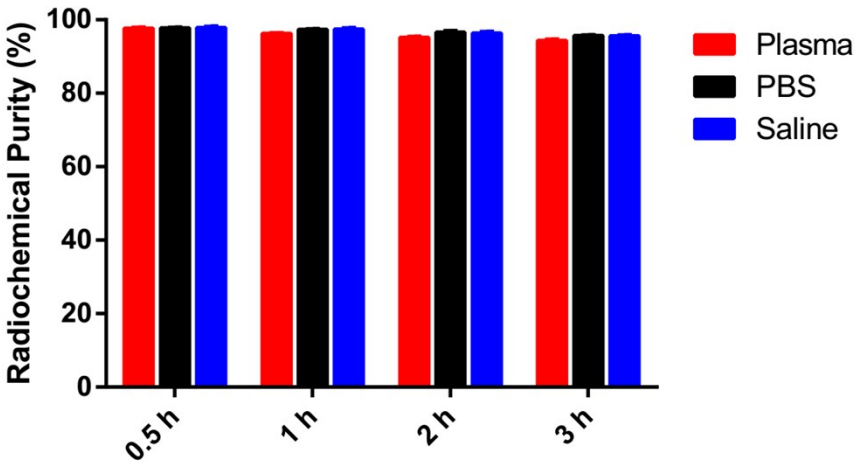

Figure S9. The stability of [^{99m}Tc]Tc-HYNIC-YQ-M3 in vitro